ISSN: 2994-9459

Research Article

Current Research in Statistics & Mathematics

Spike Generation Governed By the Stochastic Ion Adsorption-Desorption Process

Hirohisa Tamagawa[1*], Kota Ikeda[2], Bernard Delalande[3] and Titus Mulembo[4]

[1]*Department of Mechanical Engineering, Faculty of Engineering, Gifu University, 1-1 Yanagido, Gifu, Gifu, 501-1193, Japan.; BCAM, Alameda de Mazarredo 14 48009 Bilbao, Bizkaia, Spain*

[2]*School of Interdisciplinary Mathematical Sciences, Meiji University, Japan.*

[3]*280 avenue de la Pierre Dourdant, 38290, La Verpilliere, France.*

[4]*Mechatronic Engineering department, Dedan Kimathi University of Technology DEKUT, Nyeri, Kenya.*

[*]Corresponding Author
Hirohisa Tamagawa, Department of Mechanical Engineering, Faculty of Engineering, Gifu University, 1-1 Yanagido, Gifu, Gifu, 501-1193, Japan.; BCAM, Alameda de Mazarredo 1448009 Bilbao, Bizkaia, Spain

Submitted: 2023, Nov 08; **Accepted**: 2023, Nov 30; **Published**: 2023, Dec 12

Citations: Tamagawa, H., Ikeda, K., Delalande, B., Mulembo, T. (2023). Spike Generation Governed By the Stochastic Ion Adsorption-Desorption Process. *Curr Res Stat Math, 2*(1), 100-108.

Abstract

There is a deep conviction that the generation of the action potential is one of the most fundamental biological activities. According to membrane theory, active ion transport and its flow variations across the plasma membrane are responsible for generating the action potential. However, in contrast to the living model, an in vitro model based on the adsorption-desorption process of ions could explain the generation of the action potential. The authors constructed such a model and mathematically related it using the stochastic differential equation (SDE). This model is based on the ion adsorption-desorption process and SDE, and it is consistent with the kinetics of the reaction. The model could be applicable to explain the action potential generation mechanism of a living cell. We came to conclusion that it is physiologically important to reexamine the mechanism of action potential generation from the perspective of the ion adsorption-desorption model.

Keywords: Membrane Potential, Action Potential, Mass Action Law, Thermodynamics, Stochastic Process.

1. Introduction

An elucidation of the mechanism of action potential generation was a physiologically attractive and important research topic last century. Currently, all physiological textbooks refer to membrane theory to explain the mechanism of action potential generation [1–5]. The theory states that the change in the rate of ion flow across the plasma membrane is responsible for generating the action potential. Therefore, researchers agree that the generation of the action potential is fully explained by membrane theory. Several decades ago, researchers believed that they had already identified functional proteins that regulate transmembrane ion flow. These proteins are called ion channels and ion pumps. In particular, the operation of the pump is seen as an indication of life, since it consumes ATP energy. Thus, the generation of the action potential would inevitably be accompanied by a basal metabolic rate.

However, some research groups have objected to such a conventional view of the principle of action potential generation. Gilbert Ling is a leader of these researchers [4–6]. Ling presented his physiological theory called the associationinduction hypothesis (AIH). In short, the AIH attributes the generation of the action potential to the adsorption-desorption process of ions. Therefore, the phenomenon of action potential generation is not limited to living systems but can also occur in non-living systems.

Fox et al. observed a spontaneous electrical signal with artificially created microspheres [7–14]. In particular, the electrical signal of ref. [13, 14] seems indistinguishable from the action potential of a real living cell. It is therefore only natural to ask certain questions:“Is the action potential caused by transmembrane ion flow?” and “Is the action potential a consequence of vital activity?” Fox’s microspheres are mainly composed of amino acids. Therefore, it can still be argued that the microsphere is artificially created but is composed of biological substances. Therefore, some might say that the generation of an action potential is still an indication of life.

In the field of nonlinear dynamics research, the generation of action potentials of nonliving systems in aqueous solution is well known and has been studied intensively. Yoshikawa’s works are typical [15–22]. They measured the potential generated across the different artificial separators (a sort of membrane) that sep-

arated two different electrolyte solutions. They observed a frequent generation of potential peaks. To date, similar studies have been carried out by other research groups [23–28]. As another type of artificial system, corrosion is known to cause a regular generation of potential spikes [29–31]. Thus, the generation of potential peaks in the aqueous system is quite ordinary and common natural phenomenon in nonphysiological fields of science; it does not seem to require a sophisticated system.

In this paper, the generation of peak potentials observed in the metalaqueous solution system, which is an inanimate system, is shown for the first time. Then, the observed peak potential will be formulated using the stochastic model. Finally, the mechanism of action potential generation is discussed. The purpose of this work is not to be in complete denial of the current physiological model, membrane theory. However, as described above, even the broadly accepted membrane theory has faced difficulties in reasoning for some membrane potential characteristics. We suggest that the AIH-based model to be discussed in this paper could serve as an amendment to the membrane theory, if not as an alternative theory to the membrane theory.

2. Experimental Observation

First, we perform the following experiments. A metal wire was immersed in an aqueous solution of KCl and its surface potential was measured as a function of time using the setup shown in Fig.1.

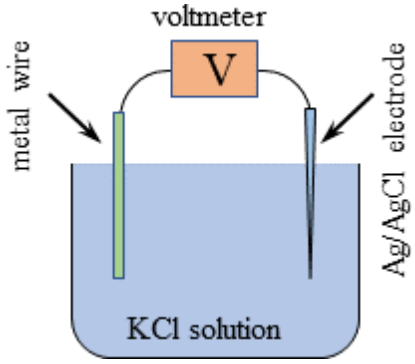

Figure 1: Experimental setup for measuring the wire surface potential A metal wire is submerged in a KCl aqueous solution.

Two types of metal wire, a nickel wire and a gold wire, were used, and Fig. 2 shows the surface potential profiles measured experimentally. The surface of the nickel wire showed continuous potential peaks, while the surface of the gold wire did not. These potential characteristics are mathematically theorized step by step in the following sections.

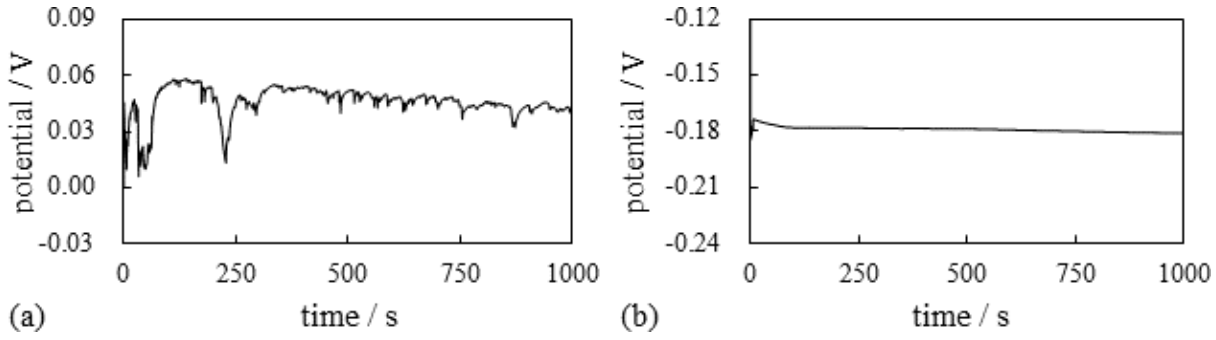

Figure 2: Experimental surface potential of a wire submerged in a 10^{-4}M KCl aqueous solution The wire used was (a) a nickel wire and (b) a gold wire

3. Potential Generation

Previous work suggests that potential characteristics are governed by adsorption of ions on the surface of the wire [32, 33]. In other words, the mobile ions *i* adsorb onto the s ion adsorption sites on the metal surface, as illustrated in Fig. 3. As the ion carries a nonzero charge, the association-dissociation between *i* and *s* results in the generation of a non-zero surface potential and its variation. This is the mechanism of membrane potential generation based on ion adsorption.

Let us see the process of generating potential peaks on the basis of the adsorption-desorption mechanism of ions. The non-zero surface potential of the wire when in contact with deionized water was experimentally observed (there are no mobile *i* ions). Therefore, in order to treat these experimental systems mathematically, we hypothesized that hypothetical charges were created on the surface of the wire when it was in an aqueous solution. We introduce ρ which represents the density of the hypothetical surface charge formed on the surface of the wire when it is immersed in deionized water.

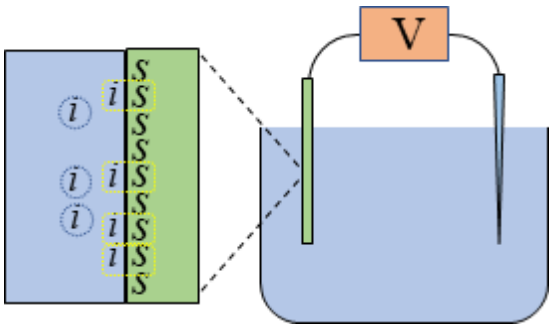

Figure 3: Association and dissociation between the metal wire surface site *s* and mobile ion *i* in the electrolytic solution *i* encircled by the dotted line represents the free *i* in the vicinity of the metal surface. *is* encircled by the dashed line represents the *is* created by the binding between *i* and *s*.

According to electromagnetism, it is easy to imagine that the charge separation between *i* and *s* generates a non-zero potential and that the combination of *i* and *s* more or less neutralizes their charges, causing a potential change. If the ion adsorption-desorption process shown in Fig. 4 occurs endlessly, the potential spike could be generated repeatedly.

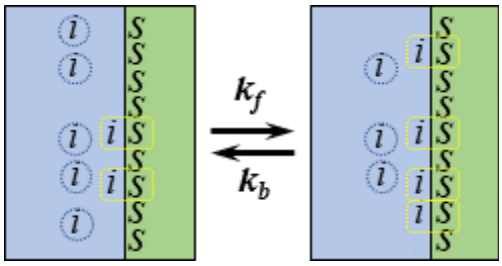

Figure 4: Adsorption-desorption process between *i* and *s*

We have assumed that the adsorption site *s* carries the charge opposite to that of the free ion *i*. Therefore, the adsorption of an *i* on an *s* results in the creation of an is that carries zero charge. In other words, the charge on *s* is neutralized by the charge on *i* due to the creation of *is*. Suppose further that the adsorption site of a single *s* ion carries a charge whose absolute value is |*e*| (*e*: elementary charge), the site density of the total adsorption site, S_T, can be given by Eq.1.

$$S_T = \frac{|\rho|}{|e|} \tag{1}$$

We introduce here S_s and S_{is} which represent the densities of the unoccupied adsorption site *s* and the occupied site *s* (i.e. *is*), respectively. S_s and S_{is} suffice to Eq.2. In summary, an occupied *s* (i.e. *is*) carries a zero charge, while an unoccupied *s* carries a non-zero charge. Thus, S_s (or S_T - S_{is}) governs the characteristics of the metal surface potential.

$$S_T = S_S + S_{is} \tag{2}$$

4. Mathematical Formula

Based on the concept introduced in the previous section, we have mathematically theorized the potential spike generation mechanism as follows:

Assuming that the ion adsorption-desorption phenomenon on the surface of the metal wire is a stochastic process, a formula is derived representing the quantity of *s*. The association and dissociation between *s* and *i* is given by Eq.3. Hence, Eq.4 is derived from the point of view of reaction kinetics [34].

$$i + s \underset{k_b}{\overset{k_f}{\rightleftharpoons}} is \tag{3}$$

$$\frac{dS_s}{dt} = -k_f S_s C_i^o + k_b S_{si} \tag{4}$$

Figure 5 is the experimenta data shown as Fig. 2(a).

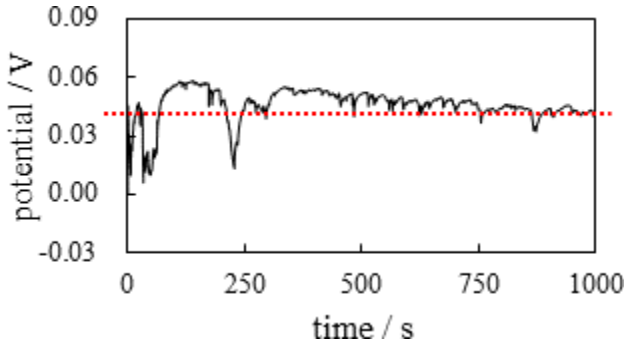

Figure 5: Nickel wire surface potential vs. time The horizontal dotted line represents the hypothetical equilibrium potential.

We speculate that these potential spikes are caused by the repetitive adsorption-desorption process of i to s and such repetitive adsorptiondesorption could be theorized in view of the stochastic process. Assuming that C_i^o consists of the equilibrium constant part, $\langle C_i \rangle_{eq}$, and the Brownian motion part, $\langle C_i \rangle_{Br}$, C_i^o is given by Eq. 5.

$$C_i^o = \langle C_i \rangle_{eq} + \langle C_i \rangle_{Br} \tag{5}$$

Given that ϕ^o represents the equilibrium metal surface potential in reference to the potential in the bulk phase of the KCl solution, $\langle C_i \rangle_{eq}$ is given by Eq. 6 according to the Boltzmann distribution where C_i^∞ and z_i represent the concentration of i in the bulk phase of the KCl solution and the valence of i, respectively [32-37]. β represents $e/(2k_BT)$: elementary charge, k_B: Boltzmann constant, T: solution temperature). We hypothesized that $\langle C_i \rangle_{Br}$ obeys the normal distribution $N(\mu,\sigma^2)$ (μ: average, σ: standard deviation). We have to add a comment on ϕ^o. The surface potential of nickel wire always fluctuates. Therefore, in reality, an equilibrium surface potential does not exist when the nickel wire is used. Therefore, in such a case, ϕ^o is hypothetical but corresponds to the potential represented by the dotted line in Fig. 5

$$\langle C_i \rangle_{eq} \equiv C_i^\infty \exp(-2z_i\beta\phi^o) \tag{6}$$

Eq. 4 can be arranged in Eq. 7 using Eq. 5.

$$\begin{aligned} \frac{dS_s}{dt} &= -k_f S_s C_i^o + k_b S_{si} \\ &= -k_f S_s(\langle C_i \rangle_{eq} + \langle C_i \rangle_{Br}) + k_b(S_T - S_s) \\ &= -(k_f \langle C_i \rangle_{eq} + k_b) S_s - k_f S_s \langle C_i \rangle_{Br} + k_b S_T \end{aligned} \tag{7}$$

Since all the quantities, k_f, k_b, $\langle C_i \rangle_{eq}$ and S_T are positive and constant, Eq. 7 can be arranged into Eq. 8 by employing P, Q, R and W defined by Eqs. 9a ~ 9c. Since dW is burdened with all the Brownian motion characteristics of $\langle C_i \rangle Brdt$, Q is inevitably considered as a negative constant quantity.

$$\begin{aligned} \frac{dS_s}{dt} &= -(k_f \langle C_i \rangle_{eq} + k_b) S_s - k_f S_s \langle C_i \rangle_{Br} + k_b S_T \\ \leftrightarrow\ dS_s &= -(k_f \langle C_i \rangle_{eq} + k_b) S_s dt + Q S_s dW + k_b S_T dt \\ \leftrightarrow\ dS_s &= P S_s dt + Q S_s dW + R dt = (R + P S_s) dt + Q S_s dW \end{aligned} \tag{8}$$

$$P \equiv -(k_f \langle C_i \rangle_{eq} + k_b) \quad (P < 0) \tag{9a}$$

$$QdW \equiv -k_f \langle C_i \rangle_{Br} dt \quad (Q < 0) \tag{9b}$$

$$R \equiv \ k_b S_T \quad (R > 0) \tag{9c}$$

Now, the calculation is performed using the Milstein scheme [38] where the time step is 0.001 s. Figure 6 shows the S_s obtained by calculation. To obtain these diagrams, the numerical values of the parameters must be determined, but it is technically impossible to do this. Therefore, as a test, we have used the Brownian motion obeying $N(0,3.0)$ (for Fig. 6 (a)) and $N(0,1.0)$ (for Fig. 6 (b)). But what numerical values are appropriate for the parameters P, Q and R? It is not permissible to choose the parameter values as one wishes, but the parameter values must be thermodynamically acceptable. As a test, we would like to use simple parameter values. For example, if Eq. 10 is established, Eq.11 could be achieved thermodynamically.

$$k_f >> k_b \tag{10}$$

$$|P| \sim |Q| \tag{11}$$

Eqs. 9b and 9c suggest that Eq. 12 can be sufficed thermodynamically since Eq. 10 establishes and the relationship between $\langle C_i \rangle_{eq}$ and $\langle C_i \rangle_{Br}$ can determine the relationship between P and Q. Therefore, we consider the simplest parameter relationship given by Eq. 13 for the following computation.

$$|P| \sim |Q| \tag{12}$$

$$|P| \sim |Q| \sim |R| \tag{13}$$

We employed the parameters P, Q, and R which are given by the constants -0.1, -0.1, and 0.05, respectively, for both Fig. 6(a) and (b). As stated at the end of the previous section "S_s (or S_T - S_{is}) governs the metal surface potential characteristics," S_s shown in Fig. 6 can qualitatively reflect the potential characteristics shown in Fig. 2. Quite intriguingly, Fig. 6 suggests that the standard deviation can rule the induction frequency of potential spike. We performed the same computation by choosing other σ numerical values and confirmed that the potential spike frequency increases by the increase of σ. Of course, there are many combinations of values for parameters (P, Q, R, μ, σ), we cannot derive the conclusion that the potential spike is in principle governed by the standard deviation σ. However, our stochastic model appears to be able to reproduce the high frequency of spike induction and the low frequency of spike induction as well. It is not against our intuition and it is not unthinkable that the surface properties of metal wire have significant influences on σ. Therefore, it is not inappropriate to say that σ is one of the governing parameters for the potential spike induction characteristics.

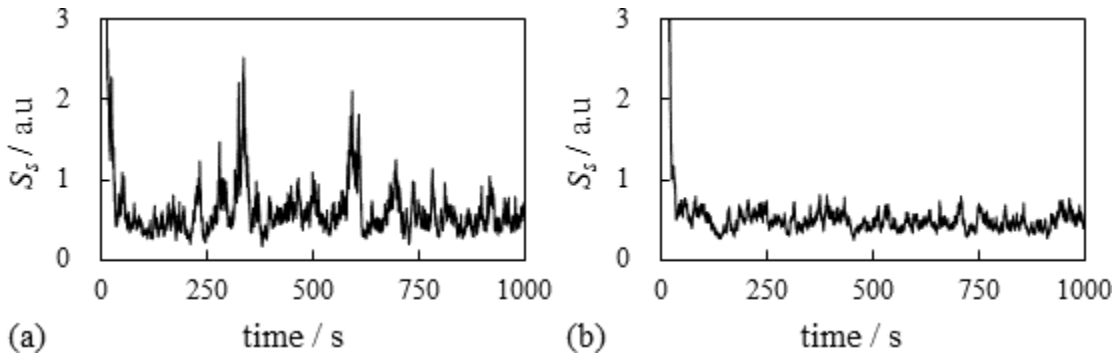

Figure 6: Computationally calculated S_s vs. time (a) $N(0,3.0)$ (b) $N(0,1.0)$ Attention: The vertical axis does not represent the quantity of S_s but the ratio of S_s.

5. S_s and Potential

How is are the characteristics of S_s related to the potential behavior mathematically? Based on prior works described in the refs. [32, 33]. The surface potential (we denote it here by Φ) and the surface charge (we denote it here by Σ) can be mathematically associated with each other as given by Eq. 14 where ϵ, ϵ_o, U_o, k_B, and T represent relative permittivity of water, vacuum permittivity, bulk phase ion concentration, Boltzmann constant, and the environmental temperature, respectively.

$$\Sigma = 2\sqrt{2\epsilon\epsilon_o U_o k_B T}\sinh(\beta\Phi) \tag{14}$$

Eq. 14 can be arranged into Eq. 15.

$$\Phi = \frac{1}{\beta}\ln\left(\frac{\Sigma}{2\sqrt{2\epsilon\epsilon_o U_o k_B T}} + \sqrt{\left(\frac{\Sigma}{2\sqrt{2\epsilon\epsilon_o U_o k_B T}}\right)^2 + 1}\right) \tag{15}$$

Tamagawa and Ikeda previously studied the relationship between the surface potential of AgCl-coated Ag wire and its surface charge density when AgCl-coated Ag wire was submerged into the electrolytic solution, and they found that Eq. 16 was established [33]. Although the experimental conditions employed in their study were different from those employed in this study, we assume that Eq. 16 is applicable to this study, too, as a test. Therefore, Eq. 15 can be approximated into Eq. 17.

$$\left(\frac{\Sigma}{2\sqrt{2\epsilon\epsilon_o U_o k_B T}}\right)^2 >> 1 \tag{16}$$

$$\Phi \sim \frac{1}{\beta}\ln\frac{\Sigma}{\sqrt{2\epsilon\epsilon_o U_o k_B T}} \tag{17}$$

Σ is proportional to Ss. Hence, Σ can be expressed by Eq.18 by introducing a constant κ. Therefore, Eq. 17 can be further arranged into Eq. 19.

$$\Sigma = \kappa S_s \tag{18}$$

$$\Phi \sim \frac{1}{\beta}\ln\frac{\Sigma}{\sqrt{2\epsilon\epsilon_o U_o k_B T}} = \frac{1}{\beta}\ln\frac{\kappa S_s}{\sqrt{2\epsilon\epsilon_o U_o k_B T}} = \frac{1}{\beta}\ln S_s + const. \tag{19}$$

Setting const. = 0 for Eq.19, Φ was computed by plugging the numerical data of S_s of Fig. 6(a), and the outcome is shown in Fig. 7. So, the spike is generated. Although the experimental data shown in Fig. 5 shows that the potential spikes are all negative going, the computationally obtained spikes shown in Fig. 7 look positive going. It appears to be a serious mismatch between the experiment and the theory. However, the sign of potential is not an essential factor in this work at all. Whether the potential spikes are positive going or negative going depends merely on the sign of charges *i* bears and *s* bears. Once the sign of their charge becomes opposite, the sign of potential becomes opposite.

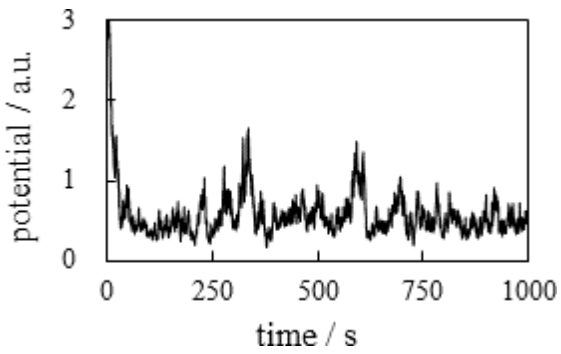

Figure 7: Computationally obtained potential by converting the data of S_s in Fig. 6(a) Attention: The vertical axis does not represent the potential but the ratio of potential.

One may say that the potential profile shown in Fig. 7 exhibits too high potential spike frequency compared with the actual experimental data in Fig. 2(a). But as stated earlier, we found that the potential spike frequency can change in accordance with the numerical value of σ. Our emphasis here does not lie in that our theoretical model can quantitatively reproduce the experimental potential profiles but in that the potential characteristics could be stochastically determined. Figure 8 shows the potential profiles of the time t = 100s ~ 250s (time range was chosen unintentionally) when $N(\mu,\sigma) = N(0,3.0)$, $N(0,1.0)$ and $N(0,0.5)$, is a clear example that the frequency of the articulate potential spikes increases with the increase of σ, though all the profiles exhibit the small fluctuation continuously.

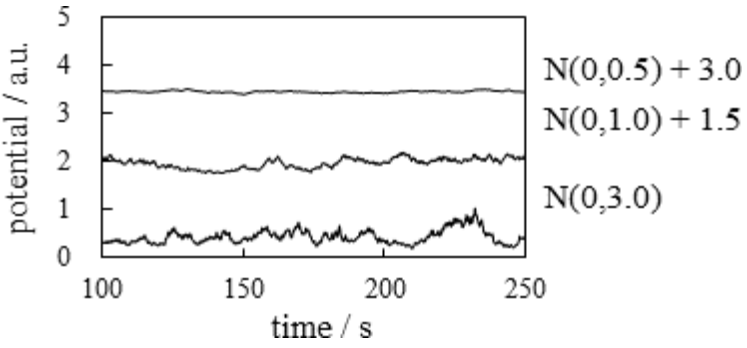

Figure 8: Computationally obtained potential profiles for (a) $N(0,3.0)$ (b) $N(0,1.0)$ (c) $N(0,0.5)$ The profiles for $N(0,1.0)$ and $N(0,0.5)$ are shifted upward by +1.5 and +3.0, respectively, so that the profiles do not overlap one another.

Furthermore, we even observed that the high frequency of potential spike can be experimentally achieved by employing a different experimental condition than the condition employed for obtaining the experimental potential shown in Fig. 2(a). Fig. 9 shows the potential profile of nickel wire submerged in a 1M NaCl solution. It exhibited a higher potential spike frequency compared with the potential profile shown in Fig. 2(a). In other words, the potential characteristics predicted by our theoretical model exist in the actual experimental system.

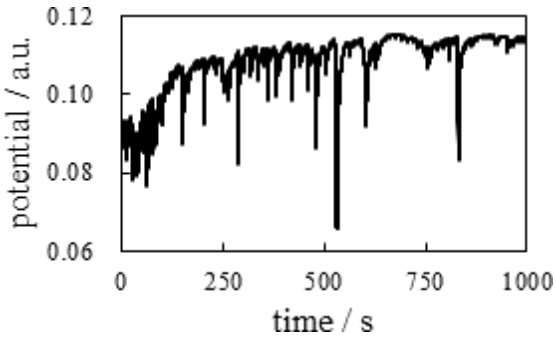

Figure 9: Experimentally measured surface potential of nickel wire submerged in a 1M NaCl solution.

The spike generation mechanism could be explained by the inanimate model based on the stochastic process. The induction of potential spikes in the living system could also be explained by this type of inanimate stochastic model. No life activity is required even for the induction of the cell's potential peak. Although the computationally obtained potential profiles are not quantitatively the same as the real experimental potential profiles, the qualitative aspects are similar to each other. Therefore, we cannot exclude the ion adsorption-desorption mechanism as a mechanism for the generation of the action potential.

6. Conclusion

The inanimate experimental system showed potential spikes, and the stochastic model reproduced the induction of potential spikes. The laws of physics never distinguish between living and nonliving systems. Therefore, it is not unusual to think that the potential spikes of a living cell can also be explained by the stochastic model. Stochastic processing of neuron activity is not new work, but such a mathematical tool has been used in the study of neuroscience [39–41] although it is not so popular. However, our way of incorporating the stochastic process into neurodynamic analysis is quite distinct from others, such as conventional work. Conventional work is a combination of ordinal neurodynamic theory and the stochastic process. The repetitive occurrence of the ion adsorption-desorption process is responsible for the generation of potential peaks in our model, and we have incorporated the stochastic process into the kinetics of the ion adsorption-desorption reaction. Our result explains the characteristics of the generation of the cellular action potential relatively well.

We understand that our model is still unable to quantitatively reproduce the regularity of real action potential characteristics. However, the simple physical process, an ion adsorption-desorption process coupled with a simple stochastic effect, can reproduce the potential spike generation computationally, though it only vaguely resembles the actual action potential. Furthermore, it has been known that there exists an irregular membrane potential, as well as a regular membrane potential [42]. Therefore, even the vague reproduction of irregular membrane potential characteristics has more or less physiological meaning and suggests the need for an amendment of the current electrophysiological model.

From our stochastic model for neurodynamics, we believe that the inanimate model should not be excluded at least as a part of the mechanism for generation of action potentials.

Declaration of COI: All the authors state that there is no conflict of interest.

References

1. Cronin, J. (1987). Mathematical aspects of Hodgkin-Huxley neural theory (No. 7). Cambridge University Press.
2. G. B. Ermentrout and D. H. Terman, Mathematical Foundations of Neuroscience (Interdisciplinary Applied Mathematics Book 35), Springer, New York, 2010.
3. J. Keener and J. Sneyd, Mathematical Physiology: I: Cellular Physiology (Interdisciplinary Applied Mathematics), Springer, New York, 2008.
4. Ling, G. N. (1992). A Revolution in the Physiology of the Living Cell.
5. Ling, G. N. (2001). Life at the cell and below-cell level: The hidden history of a fundamental revolution in biology New York: Pacific Press.
6. Ling, G. N. (1997). Debunking the alleged resurrection of the sodium pump hypothesis. Physiological chemistry and physics and medical NMR, 29(2), 123-198.
7. Ishima, Y., Przybylski, A. T., & Fox, S. W. (1981). Electrical membrane phenomena in spherules from proteinoid and lecithin. BioSystems, 13(4), 243-251.
8. Przybylski, A. T., Stratten, W. P., Syren, R. M., & Fox, S. W. (1982). Membrane, action, and oscillatory potentials in simulated protocells. Naturwissenschaften, 69(12), 561-563.
9. Przybylski, A. T., & Fox, S. W. (1984). Excitable artificial cells of proteinoid. Applied Biochemistry and Biotechnology, 10, 301-307.
10. Matsuno, K. (1984). Electrical excitability of proteinoid microspheres composed of basic and acidic proteinoids. BioSystems, 17(1), 11-14.
11. Przybylski, A. T. (1985). Excitable cell made of thermal proteinoids. BioSystems, 17(4), 281-288.
12. Vaughan, G., Przybylski, A. T., & Fox, S. W. (1987). Thermal proteinoids as excitability-inducing materials. BioSystems, 20(3), 219-223.
13. K. Haefner, (Ed). (1992). Evolution of Information Processing Systems An Interdisciplinary Approach for a New Understanding of Nature and Society, Springer, New York.
14. Fox, S. W., Bahn, P. R., Dose, K., Harada, K., Hsu, L., Ishima, Y., ... & Yu, B. (1995). Experimental retracement of the origins of a protocell: it was also a protoneuron. Journal of biological physics, 20(1-4), 17-36.
15. Yoshikawa, K., & Matsubara, Y. (1983). Spontaneous oscillation of electrical potential across organic liquid membranes. Biophysical Chemistry, 17(3), 183-185.
16. Yoshikawa, K., Sakabe, K., Matsubara, Y., & Ota, T. (1984). Oscillation of electrical potential in a porous membrane doped with glycerol α-monooleate induced by an Na+/K+ concentration gradient. Biophysical chemistry, 20(1-2), 107-109.
17. Yoshikawa, K., Sakabe, K., Matsubara, Y., & Ota, T. (1985). Self-excitation in a porous membrane doped with sorbitan monooleate (Span-80) induced by an Na+/K+ concentration gradient. Biophysical chemistry, 21(1), 33-39.
18. Toko, K., Yoshikawa, K., Tsukiji, M., Nosaka, M., & Yamafuji, K. (1985). On the oscillatory phenomenon in an oil/water interface. Biophysical Chemistry, 22(3), 151-158.
19. Yoshikawa, K., Omochi, T., & Matsubara, Y. (1986). Chemoreception of sugars by an excitable liquid membrane. Biophysical Chemistry, 23(3-4), 211-214.
20. Yoshikawa, K., Omochi, T., Matsubara, Y., & Kourai, H. (1986). A possibility to recognize chirality by an excitable artificial liquid membrane. Biophysical Chemistry, 24(2), 111-119.
21. Yoshikawa, K., Shoji, M., Nakata, S., Maeda, S., & Kawakami, H. (1988). An excitable liquid membrane possibly mimicking the sensing mechanism of taste. Langmuir, 4(3), 759-762.

22. Nakajo, N., Yoshikawa, K., Shoji, M., & Ueda, I. (1990). Spontaneous oscillation of artificial membrane: Equivalence in effects of temperature and volatile anesthetic. Biochemical and biophysical research communications, 167(2), 450-456.
23. Saito, M., Koyano, T., Miyamoto, Y., Kaifu, K., Kato, M., & Kawamura, K. (1990). Electric Self-sustained Oscillations of a DOPH-Millipore Membrane induced by Acid. Membrane, 15, 228-230.
24. Srividhya, J., & Gopinathan, M. S. (2003). Modeling experimental oscillations in liquid membranes with delay equations. The Journal of Physical Chemistry B, 107(6), 1438-1443.
25. Gao, J., Wang, L., Yang, W., & Yang, F. (2005). Electrical potential oscillation in an anionic surfactant system with barbitone in octanol as an oil phase. Journal of the Iranian Chemical Society, 2, 71-77.
26. Ogawa, T., Shimazaki, H., Aoyagi, S., & Sakai, K. (2006). Novel modeling of electrical potential oscillation across a water/octanol/water liquid membrane. Journal of membrane science, 285(1-2), 120-125.
27. Gao, J. Z., Dai, H. X., Chen, H., Ren, J., & Yang, W. (2007). Study on the oscillating phenomena of electrical potential across a liquid membrane. Chinese Chemical Letters, 18(3), 309-312.
28. Kovalchuk, N. (2015). Spontaneous non-linear oscillations of interfacial tension at oil/water interface. Open Chem 13: 1–16.
29. Li, Y., Ives, M. B., & Coley, K. S. (2006). Corrosion potential oscillation of stainless steel in concentrated sulphuric acid: I. Electrochemical aspects. Corrosion science, 48(6), 1560-1570.
30. Jones, S., Li, Y., Coley, K. S., Kish, J. R., & Ives, M. B. (2010). Corrosion potential oscillations of nickel-containing stainless steel in concentrated sulphuric acid: II Mechanism and kinetic modelling. Corrosion science, 52(1), 250-254.
31. Sazou, D., Pavlidou, M., & Pagitsas, M. (2012). Potential oscillations induced by localized corrosion of the passivity on iron in halide-containing sulfuric acid media as a probe for a comparative study of the halide effect. Journal of Electroanalytical Chemistry, 675, 54-67.
32. Tamagawa, H. (2019). Mathematical expression of membrane potential based on Ling's adsorption theory is approximately the same as the Goldman–Hodgkin–Katz equation. Journal of Biological Physics, 45, 13-30.
33. Tamagawa, H., & Ikeda, K. (2018). Another interpretation of the Goldman–Hodgkin–Katz equation based on Ling's adsorption theory. European Biophysics Journal, 47, 869-879.
34. G. M. Barrow. (1984). Physical Chemistry, McGraw-Hill Inc., New York.
35. Kitahara, A., & Watanabe, A. (Eds.). (1984). Electrical phenomena at interfaces: Fundamentals, Measurements, and Applications (Vol. 15). M. Dekker.
36. Bockris, J. O. M., & Khan, S. U. (1993). Surface Electrochemistry: A Molecular Level Approach. Springer Science & Business Media.
37. C. M. A. Brett and A. M. O. Brett. (1993). Electrochemistry Principles, Methods and Applications, Oxford University Press, New York.
38. Kloeden, P. E., & Platen, E. (1992). Higher-order implicit strong numerical schemes for stochastic differential equations. Journal of statistical physics, 66, 283-314.
39. P. Holmes, E. Brown, J. Moehlis, R. Bogacz, J. Gao, P. Hu, G. AstonJones, E. Clayton, J. Rajkowski and J.D. Cohen, Optimal decisions: From neural spikes, through stochastic differential equations, to behavior, 2004 International Symposium on Nonlinear Theory and its Applications (NOLTA2004), Fukuoka, Japan, Nov. 29 - Dec. 3, 2004.
40. Goldwyn, J. H., Imennov, N. S., Famulare, M., & Shea-Brown, E. (2011). Stochastic differential equation models for ion channel noise in Hodgkin-Huxley neurons. Physical Review E, 83(4), 041908.
41. Rowat, P. F., & Greenwood, P. E. (2014). The ISI distribution of the stochastic Hodgkin-Huxley neuron. Frontiers in Computational Neuroscience, 8, 111.
42. We refrain from citing particular papers about the generation of irregular membrane potential since a great number of literature are available about it.